QUIET DRONES 2026
Delft, 29th June - 1st July 2026

Effect of propeller blade spacing on a quadcopter's sound quality

Session: Experimental Aeroacoustic Measurements – Field

Carlos Ramos-Romero[1*], *Dima Usov*[2], *Antonio Filippone*[2], *and Antonio J. Torija*[1]

[1]Acoustics Research Centre, The University of Salford, Salford M5 4WT, UK.
[2]School of Engineering, The University of Manchester, Manchester M13 9PL, UK.
[*]c.a.ramosromero@salford.ac.uk

Abstract It is well known that propeller and blade geometry are the main contributors to aeroacoustic noise in propeller-driven vehicles. This paper investigates how the acoustic emissions and the sound quality of a quadcopter are affected when it is equipped with two propeller sets that are aerodynamically similar but differ in geometry. An outdoor measurement campaign was conducted to characterise the acoustic response of the vehicle operating with two aerodynamically equivalent, two-bladed, low-Reynolds-number propeller sets with different blade spacing angles. The acoustic energy distribution across the frequency spectrum induced by propeller geometry is examined for static flight operations. By keeping constant operational conditions (i.e., altitude, flight speed and payload) and design parameters (e.g., number of blades and motors, and vehicle mass), significant differences in the emitted noise were observed for propellers with different blade-spacing angles. These operations were characterised using a set of overall acoustic descriptors (LA_{max}, LA_{eq}, LA_E) and spectral analysis. A shift of acoustic energy toward the low-frequency range and a redistribution of harmonics were observed when the vehicle operated with the altered blade-spacing-angle propeller compared with the baseline propeller configuration. Moreover, this acoustic spectral redistribution mainly affects the psychoacoustic assessment of roughness and tonality; meanwhile, loudness, fluctuation strength, and sharpness exhibit negligible changes.

Keywords: quadcopter, asymmetric propellers; acoustic characterisation.

1. Introduction

The rapid expansion of Uncrewed Aerial Systems (UAS) and the emergence of Advanced Air Mobility (AAM) are reshaping the modern aviation market. As operational activity increases, the environmental and societal impacts, particularly noise impact and annoyance, require further investigation (Schäffer, Pieren, Heutschi, Wunderli, & Becker, 2021).

In response to these concerns, aviation authorities and regulatory agencies are actively developing certification frameworks for UAS and eVTOL acoustic emissions (Civil Aviation Authority, 2023; European Union Aviation Safety Agency, 2023; Federal Aviation Administration, 2023). These emerging standards place increasing emphasis on integrating low-noise strategies early in the design process. Therefore, understanding and controlling propeller noise generation mechanisms is a critical enabler for the sustainable deployment of aerial robotics for AAM services.

Conventional rotary-wing designs are typically azimuthally symmetric, with identical blades evenly distributed around azimuth. Such configurations offer clear advantages, including smooth thrust output, structural balance, simplified manufacturing, well-established theoretical and experimental foundation. However, symmetry inherently concentrates acoustic energy at the blade-passing frequency (BPF) and its harmonics, producing strong tonal signatures that are known to have detrimental effects on the perceived annoyance. An alternative approach is to intentionally break radial symmetry through uneven blade spacing or non-identical blade geometries. Introducing asymmetry modifies the temporal loading distribution and redistributes acoustic energy across a broader frequency range (Sonneborn & Drees, 1975; Dobrzynski, 1993; Iannotta et al., 2025). Previous experimental investigations by the authors (Usov et al., 2024; Usov, Chronis, & Filippone, 2025) showcased that asymmetric propellers with uneven blade spacing can redistribute the acoustic energy spectrum, while maintaining comparable aerodynamic performance. However, the effects on the sound quality of a UAS equipped with asymmetric propellers have not yet been investigated.

Building on these previous studies, the present work examines the effect of uneven blade spacing on the acoustic and psychoacoustic features of a quadcopter operating outdoors. An experimental measurement campaign was performed using two aerodynamically similar, two-bladed, low-Reynolds-number propeller sets: a conventional symmetric and an azimuthally asymmetric. Acoustic measurements were obtained from a representative static-flight manoeuvre to characterise how blade-spacing asymmetry modifies the vehicle noise in terms of spectral content, overall acoustic metrics, and sound-quality metrics. The vehicle mass, flight trajectory, and operating conditions were maintained consistently. The flight-log analysis confirmed that the asymmetric propeller did not measurably affect the operational performance of the vehicle.

2. Experimental Setup

2.1 Propeller design

Two propeller configurations were used in the experiments. The baseline configuration (Prop R) corresponds to a typical symmetric two-bladed 16x5.5-inch folding propeller with conventional 180-degree blade spacing. The second configuration (Prop V) introduces an azimuthal asymmetry, with blades separated by 90-degree angles. Figure 1 shows the propeller sets with identical blades. The blades share the same geometric parameters, including radius, pitch, planform, and airfoil distribution. The blade-spacing angle is therefore the primary geometric design variable considered in this study.

A detailed description of the propeller geometry, as well as their free-field acoustics characteristics and aerodynamic response, can be found in (Usov, Koning, Filippone, Poggi, & Bernardini, 2026; Usov et al., 2025). Due to a requirement for a counterweight, each asymmetric propeller was approximately 50 g heavier than the corresponding baseline propeller. To maintain the same total vehicle weight and disk loading between two propeller sets, a 200 g ballast mass was added to the UAS when operating with the baseline propellers, corresponding to the mass difference across the four rotors.

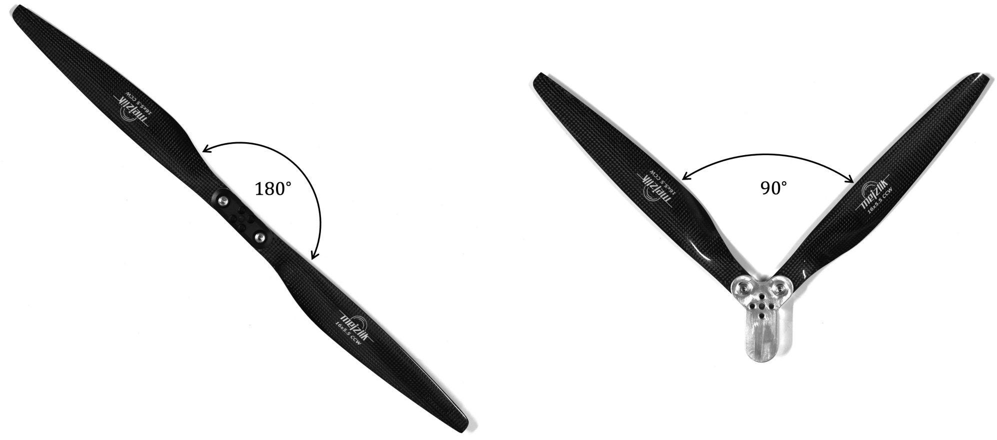

(a) Symmetric propeller, Prop R

(b) Asymmetric propeller, Prop V

Figure 1: Propeller configurations used in the experiments. (a) Baseline symmetric two-bladed propeller, denoted Prop R, with conventional 180° blade spacing. (b) Azimuthally asymmetric two-bladed propeller, denoted Prop V, with 90° blade spacing. Both propeller sets use identical blades and share the same radius, pitch, planform, and airfoil distribution.

2.2 UAS and flight trajectory

The UAS used in these experiments was a custom-built autonomous quadcopter described in (Koning, Usov, Ramos-Romero, & Filippone, 2024). The UAS is depicted in Figure 2 and its primary specifications are summarised in Table 1. During the experiments, the total operating mass of the UAS was maintained at 3420 g.

Figure 2: Photograph of the experimental UAS platform used in the experiments. The vehicle appears equipped with a set of asymmetric propellers.

Table 1: UAS specifications.

Parameter	Unit	Value
Operating weight W_0	g	3420
Propeller tip-radius	mm	203.2
Propeller pitch	mm	139.7
Frame size	mm	690.0
Disk Loading at W_0	Nm^{-2}	65

The Γ-shape flight trajectory, consisting of take-off, hover, and landing phases, is shown in Figure 3a. This trajectory has been considered as a simulated manoeuvre for facilities inspection purposes (Read, Senzig, Cutler, Elmore, & He, 2020). The take-off regime corresponds to the flight trajectory from the take-off point A to the hover position at point D, passing through the intermediate waypoint C. Acoustic measurements were initiated at propeller spin-up at point A. The hover regime corresponds to stationary flight at point D, where the vehicle maintained a fixed position relative to the ground. The landing operation corresponds to the descent from point C to the ground. The intermediate point B was used as a reference point for the landing operation, at which the vehicle passed the 10 m altitude mark, and the measurements terminated immediately after touchdown at point A. In this paper, the 20 s recording segments corresponding to the hovering regime were analysed.

The trajectory was predefined using a mission planner and maintained constant across all test cases to ensure repeatable operating conditions. Onboard systems parameters were recorded during the flight, including measurements from the GPS, barometer, and inertial measurement unit (IMU). Flight data and acoustic measurements were time-synchronised. All three operating regimes were performed within a single flight. Identical flight trajectories and control settings were used for both propeller configurations. Each test case was recorded at least 3 times to ensure repeatability of both flight trajectories and the acoustic measurements.

The performance of the UAS during hovering was also compared between tests conducted using Prop V and Prop R. The analysed flight metrics include altitude, attitude, and velocity. This comparison aims to quantify the discrepancies in operational behaviour between the asymmetric and conventional propellers and support the interpretation of the measured acoustic response.

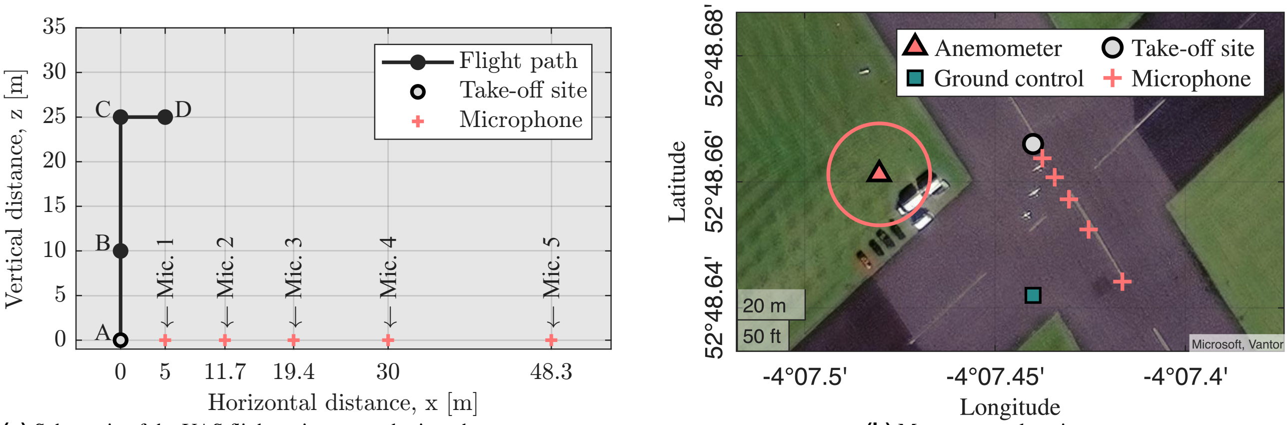

(a) Schematic of the UAS flight trajectory and microphone arrangement **(b)** Measurement location

Figure 3: Test site and source–receiver schematics. (a) Γ-shaped manoeuvring and microphone positions; (b) measurement location at the intersection of two runways.

2.3 Test site and microphone's setup

Flight tests were conducted at the Snowdonia Aerospace Centre, Llanbedr, Wales. The location provides low background noise due to its remoteness from major road traffic and commercial air corridors.

Five inverted microphones (GRAS 46AO 1/2" CCP Pressure Standard Microphone Set) were mounted on tripods at a height of exactly 7 mm above the steel-plate surface installed as the half-array configuration recommended by the BS ISO 5305:2004 standard. The microphones were arranged at 15° intervals from the vertical axis, with the vehicle positioned at a maximum altitude of 25 m above ground level (see Fig.3a). Acoustic measurements were acquired synchronously at a 50 kHz sample rate by a multi-channel data acquisition system Dewesoft SIRIUSi unit. All microphones were equipped with foam windshields to minimise wind-induced flow noise.

The acoustic measurements were performed at the intersection of two runways, as shown in Figure 3b. Background spectral levels measured before flight operations remained below 38 dBA, indicating favourable environmental conditions for acoustic measurements. The primary background noise sources were occasional aircraft flyovers, bird chirps, and trains passing along a railway located approximately one kilometre east of the test site. Wind conditions recorded during the measurement campaign reported constant wind direction with a mean wind speed of approximately 4 m/s and gusts up to 6 m/s heading north.

3. Reesults and Discussion

3.1 Flight logs

Flight logs were analysed to verify the repeatability of the flight conditions and ensure consistency between test cases. As shown in Figure 4, the altitude, velocity, and attitude time histories ($\pm\sigma$) exhibit closely overlapping trends for both propeller configurations during the hovering operation. Attitude is expressed in terms of roll (ϕ), pitch (θ), and yaw (ψ) angles in radians. The time histories of altitude, velocity, and attitude shown for hovering correspond to the time window bounded by t_0 and t_1, which defines the 20 s segment used for acoustic evaluation.

No significant deviations were observed between Prop R and Prop V, indicating consistent static flight conditions and vehicle dynamic response throughout the tests. These results confirm that the operating state of the vehicle, together with the stable low-wind conditions, was effectively identical for both propeller configurations during the analysed measurement segments. Consequently, any observed differences in the acoustic response can be primarily attributed to changes in propeller geometry rather than variations in flight dynamics.

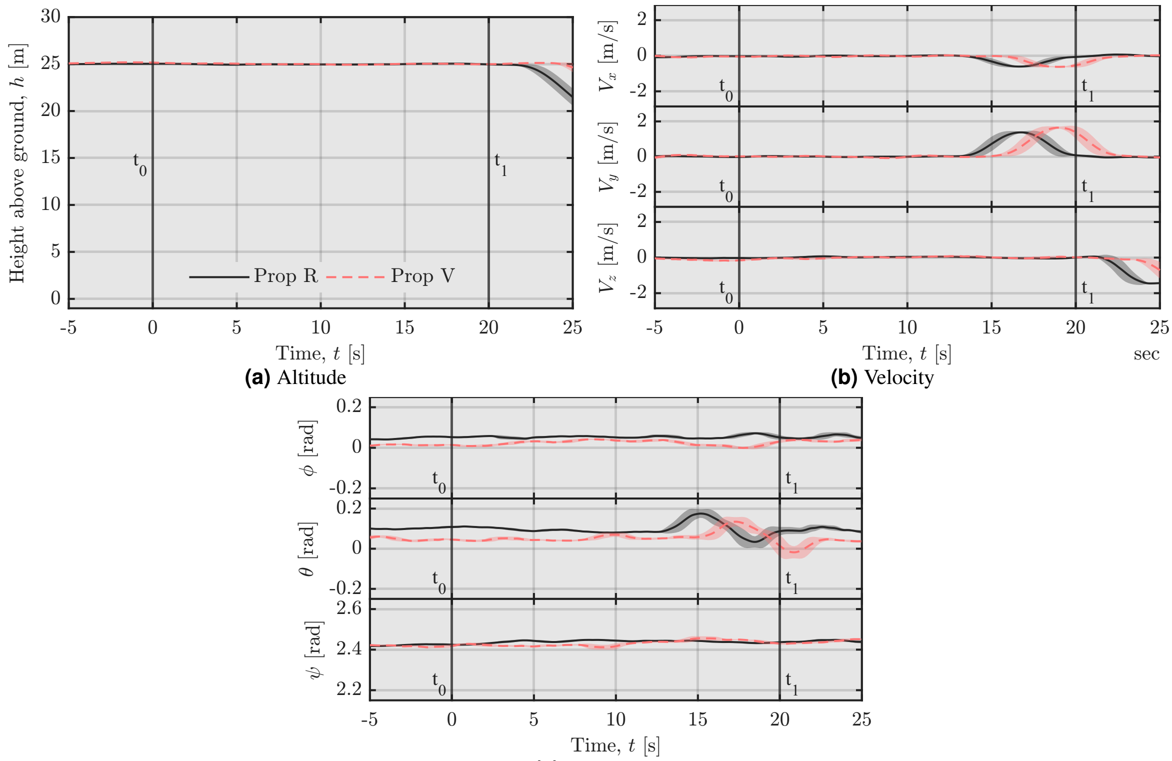

(a) Altitude

(b) Velocity

(c) Attitude

Figure 4: Flight logs of (a) altitude, (b) velocity, and (c) attitude time histories ($\pm\sigma$) comparing Prop R and Prop V configurations for the hovering operation.

3.2 Aeroacoustic noise

This section compares the aeroacoustic noise of the tested propeller sets during hovering.

The spectrograms calculated from the signals gathered by the microphone 1 are presented in Figure 5a and 5b. Since the number of blades is identical for both propeller types, the number of loading and thickness aeroacoustic sources remains unaltered. The unevenly spaced propeller (Prop V) design seems to produce a frequency shift effect, which is combined with a reduction in the amplitude of the BPF harmonics (e.g., between 100 and 500 Hz).

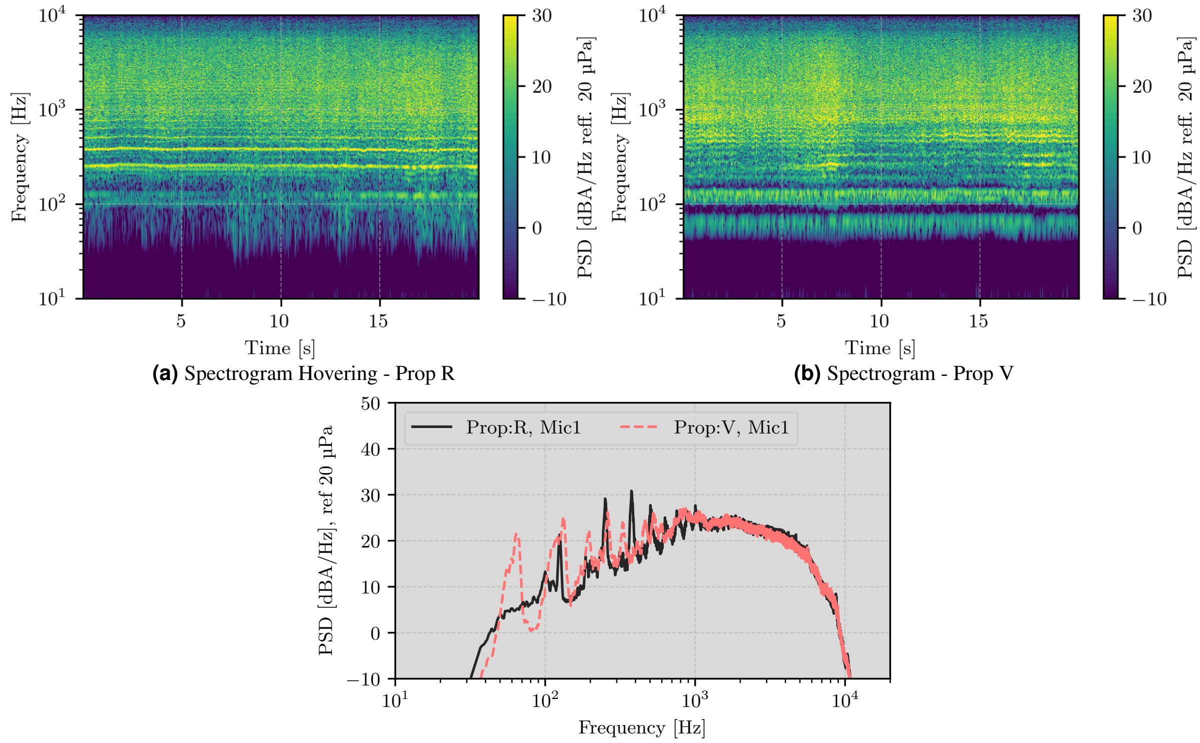

(a) Spectrogram Hovering - Prop R

(b) Spectrogram - Prop V

(c) PSD - Hovering

Figure 5: Spectrograms of the quadcopter equipped with the baseline Prop R propeller set (a) and the asymmetric Prop V propeller set (b), and Power spectral density plot comparing both propeller sets (c) during hovering operation. Plotted data were recorded at the microphone 1 position.

The PSD plot in Figure 5c clearly illustrates the differences in frequency content resulting from the change in propellers. The frequencies that initially had the highest amplitudes for Prop R show reduced amplitudes for Prop V. PSD show a redistribution of the tonal components towards the low frequencies when the vehicle operates with Prop V. The BPF of Prop R is equal to the second tone ($2 \times$ BPF) of Prop V. During the hovering regime, the high-frequency broadband noise remains largely unchanged above 1 kHz, regardless of the propeller type used.

Table 2 presents the pressure-based acoustic metrics across all microphone positions for Prop R and Prop V during the hovering regime. The pressure-based metrics show minimum differences of approximately 1 dB when comparing both propeller types at each microphone position. Interestingly, these results demonstrate comparable noise emission levels for both propeller types, despite the variations in pitch and intensity observed in the spectrograms and PSD plot.

From the spectrogram, it can be inferred that the BPF of Prop R is located around 110 Hz, whereas the vehicle operating with Prop V shifts the fundamental tone down to 75 Hz. The uneven blade spacing alters the natural propeller's distribution for harmonics (i.e., integer$\times$BPF). For the tested asymmetric propeller, the harmonics seem to be allocated at odd-integer frequencies (i.e., integer$\times$0.5$\times$BPF). As a result, Prop V tones appear to be closer to each other. Consequently, changes in the sound perception should be expected and will be discussed in the following subsection.

The sound recordings during the hovering operation allowed the directivity analysis by back-propagating the signals at a constant radius. The pressure-based metrics are then calculated at 10 m radius around the source. Figure 6 shows directivity plots confirming a similar acoustic emission for both propellers when the source is evaluated by continuous equivalent SPL (LA_{eq}) and sound exposure level (LA_E). However, Propeller V generates slightly higher ($\sim$2.5dB) maximum SPL (LA_{max}) at all angles.

Table 2: Pressure-based metrics across five microphone positions for Propeller types R and V during hovering. Values are presented as mean ± standard deviation (σ) in dBA.

		Mic 1		Mic 2		Mic 3		Mic 4		Mic 5	
Propeller	Metric	Level	$\pm\sigma$	Level	$\pm\sigma$	Level	$\pm\sigma$	Level	$\pm\sigma$	Level	$\pm\sigma$
R	LA_{max}	60.3	0.6	59.2	0.9	56.5	0.9	52.4	0.8	46.6	0.8
	LA_{eq}	57.9	0.4	56.8	0.4	53.6	0.6	49.1	0.5	43.8	0.2
	LA_E	70.9	0.4	69.8	0.4	66.6	0.6	62.1	0.5	56.9	0.2
V	LA_{max}	61.3	0.2	60.1	0.6	57.3	0.9	53.1	0.8	47.5	0.2
	LA_{eq}	57.9	0.5	56.7	0.6	53.1	0.5	49.5	0.4	44.7	0.3
	LA_E	70.9	0.5	69.7	0.6	66.2	0.5	62.4	0.4	57.7	0.3

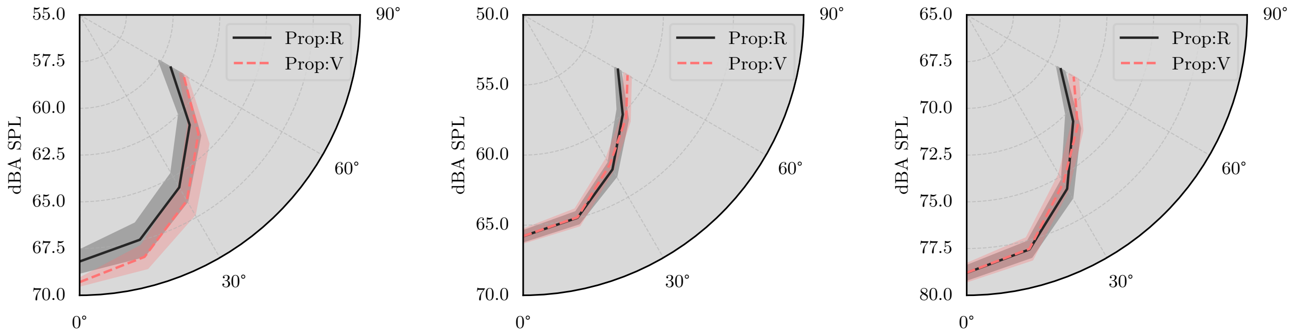

(a) LA_{max} (b) LA_{eq} (c) LA_E

Figure 6: Directivity for pressure-based metrics for Hovering. The polat plots depict the metrics for the acoustic signals that were backpropagated at a 10 m radius from the UAS.

3.3 Sound quality analysis

Those changes in sound quality can be assessed using psychoacoustic Sound Quality Metrics (SQMs). The evaluated SQMs include Sottek's Hearing Model (SHM) metrics by ECMA-418-2:2022, namely loudness, tonality, roughness, and fluctuation strength, as well as sharpness by DIN 45692 model (ECMA International, 2022; Becker, Sottek, & Lobato, 2022; DIN-45692, 2009). In addition, by combining these SQMs, the psychoacoustic annoyance (PA) can also be estimated by Eq. 1. A modified version of the PA model developed by NASA is adopted, in which SHM loudness is used instead of the original DIN loudness metric (Boucher et al., 2024).

$$PA_{NASA} = N\left(1+\sqrt{w_S^2+w_{FR}^2+w_T^2}\right) \quad (1)$$

, where the SQMs terms w were calculated with the 5% exceedance values of all the SQMs, as follows: $w_S = (S-1.75)\times 0.25\log_{10}(N+10)$ if $S > 1.75$ ($w_S = 0$ otherwise), $w_{FR} = \frac{2.18}{N^{0.4}}(0.4F+0.6R)$, and $w_T = 3.2\frac{T}{N_5}$. Figure 7 presents a comparison of the tested propeller types by means of the psychoacoustic assessment at each microphone position during hovering operation.

Loudness SHM shows minimum differences between propellers. This result highly correlates with the behaviour of $L_{A,eq}$ presented in Table 2. Prop V seems to present the lower tonality SHM across all the microphone positions. This behaviour of tonality on static flight regime correlates with the broader tones of Propeller V compared to the narrower BPF harmonics of Propeller R (See Fig. 5). The asymmetric spacing of Prop V exhibits the highest roughness SHM values across all microphone positions. Compared with the regular propeller, the additional odd harmonic tones generated by Prop V increase tone–tone interactions, resulting in rapid amplitude fluctuations characteristic of a rough sound. In

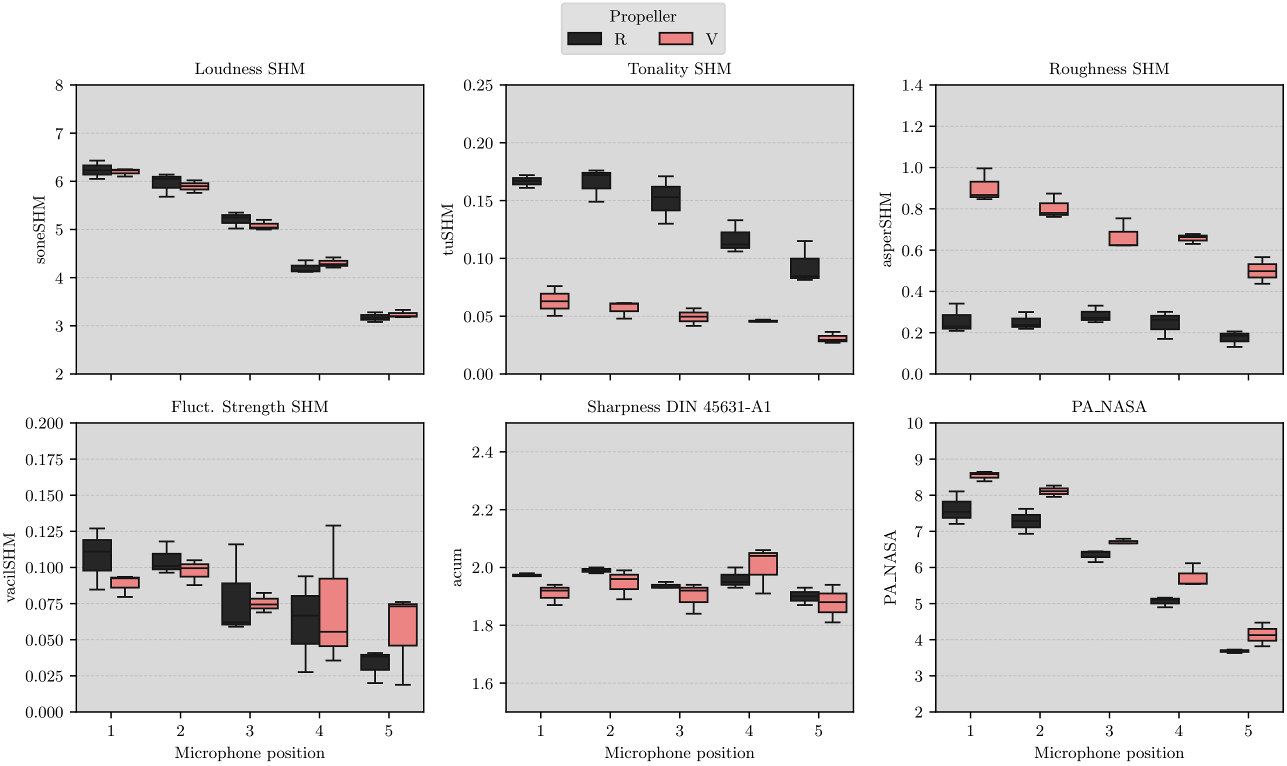

Figure 7: Box plot comparison of the symmetric (Prop R) and asymmetric (Prop V) propellers using Psychoacoustic Sound Quality Metrics and Psychoacoustic Annoyance evaluated at all microphone positions during hovering.

contrast, the slow amplitude modulations associated with fluctuation strength SHM show similar behaviour for both propeller types; however, the increased variability with distance may be affected by the low-frequency energy content of the background noise. The relatively equal contributions of high-frequency noise from both types of propellers are shown in the sharpness DIN plot. This result correlates with the similar high frequency response for both propeller types presented in Figure 5. The estimated psychoacoustic annoyance at all microphone positions is presented in Figure 7 (bottom right panel). The vehicle equipped with Prop V exhibits a more annoying sound quality character. The main factors differentiating the tested propeller types, contributing to variations in psychoacoustic annoyance, appear to be primarily roughness and tonality.

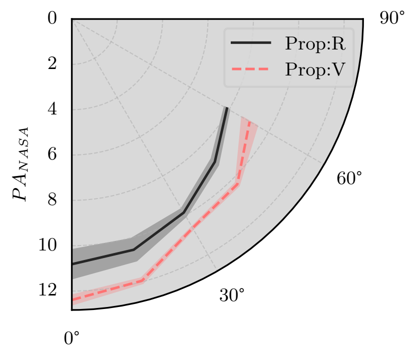

Figure 8: Directivity of psychoacoustic annoyance for propeller configurations Prop R and Prop V during hovering. PA values are calculated from signals back-propagated to a reference distance of 10 m from the source.

In addition, from the back-propagated signals at a constant radius of 10 m, it was also possible to calculate the PA around the source. Figure 8 shows that Prop V is estimated to be more annoying at all studied angles of incidence. In contrast to the pressure-based acoustic metrics, especially L_{Aeq}, where equal directivity is reported for both propeller types (see Fig. 6).

4. Conclusion

This study investigated the effect of propeller blade-spacing angle on the aeroacoustic and sound quality response of a quadcopter operating outdoors. Two aerodynamically similar two-bladed propeller configurations were compared: a baseline symmetric (Prop R) and an azimuthally asymmetric configuration (Prop V). The asymmetric propeller configuration did not measurably alter the operational behaviour of the vehicle.

The aeroacoustic analysis shows that both propeller configurations produce comparable overall sound pressure levels, despite clear differences in their spectral distribution. The spectrograms and PSD reveal a clear redistribution of tonal energy for the asymmetric propellers. Nevertheless, the high-frequency broadband content above 1 kHz remains largely unaffected by the propeller configuration, indicating that the observed differences are primarily related to tonal rather than broadband mechanisms.

From a psychoacoustic perspective, these spectral modifications translate into perceptible changes in sound quality, even if overall SPL remains similar. Prop V increases roughness and reduces tonality compared with Prop R, consistent with the presence of additional harmonic interactions and closer spectral spacing. Fluctuation strength and sharpness, however, remain largely comparable between configurations, suggesting limited impact on slow amplitude modulations and high-frequency content. These combined effects indicate that the psychoacoustic annoyance reported for Propeller V is higher than for Prop R. It is mainly driven by increased roughness and, to a lesser extent, by reduced tonality rather than changes in high-frequency broadband noise.

Acknowledgments

This project was part-funded by the Horizon Europe - UKRI under the UK government's Horizon Europe ImAFUSA project (101114776), REFMAP project (10061935), and UKRI-EPSRC GAAPS project (EP/W010119/1). C.R-R also acknowledge the Acoustics Innovation Institute Funding Call 2026 at the University of Salford for supporting this work.

References

Becker, J., Sottek, R., & Lobato, T. (2022). Psychoacoustic modeling of fluctuation strength. In *Proceedings of fortschritte der akustik – daga 2022* (pp. 967–970). Stuttgart, Germany. Retrieved from https://pub.dega-akustik.de/DAGA_2022/data/articles/000307.pdf

Boucher, M. A., Christian, A. W., Krishnamurthy, S., Tracy, T., Begault, D. R., Shepherd, K., & Rizzi, S. A. (2024). *Toward a psychoacoustic annoyance model for urban air mobility vehicle noise.* National Aeronautics and Space Administration. Retrieved from https://ntrs.nasa.gov/citations/20240003202

Civil Aviation Authority. (2023, 3). *Noise measurements from evtol aircraft: A review of available data* (No. CAP 2506). Crawley, United Kingdom. Retrieved from https://www.caa.co.uk/our-work/publications/documents/content/cap2506/

DIN-45692. (2009). *Measurement technique for the simulation of the auditory sensation of sharpness.* Berlin, Germany. (Messtechnische Simulation der Hörempfindung Schärfe)

Dobrzynski, W. (1993). Propeller noise reduction by means of unsymmetrical blade-spacing. *J. Sound Vib.*, *163*(1), 123-126. Retrieved from https://doi.org/10.1006/jsvi.1993.1152

ECMA International. (2022). *ECMA-418-2:2022 Psychoacoustic metrics for ITT equipment — Part 2 (models based on human perception)* (Vol. ECMA Tech. Report). Retrieved from https://www.ecma-international.org/publications-and-standards/standards/ecma-418/

European Union Aviation Safety Agency. (2023, 7). *Environmental protection technical specifications applicable to vtol-capable aircraft powered by non-tilting rotors.* Cologne, Germany. Retrieved from https://www.easa.europa.eu/en/document-library/product-certification-consultations/consultation-paper-environmental-protection

Federal Aviation Administration. (2023, 7). *Advanced air mobility implementation plan.* Washington, DC. Retrieved from https://www.faa.gov/air-taxis/implementation-plan

Iannotta, M., Visingardi, A., Quagliarella, D., De Gregorio, F., Barbarino, M., & Zanotti, A. (2025). Improvement of a free-wake model for the aerodynamic and aeroacoustic analysis of a small-scale two-bladed propeller in hover. *Aerospace*, *12*(5). Retrieved from https://doi.org/10.3390/aerospace12010005

Koning, D., Usov, D., Ramos-Romero, C., & Filippone, A. (2024). Flight performance and acoustics of asymmetric propellers with uneven blade spacing. In *Quiet drones 2024.* Manchester, United Kingdom. Retrieved from https://doi.org/10.17866/rd.salford.27886224

Read, D. R., Senzig, D. A., Cutler, C. J., Elmore, E., & He, H. (2020). *Noise measurement report: Unconventional aircraft – choctaw nation of oklahoma: July 2019* (Tech. Rep. No. DOT-VNTSC-FAA-20-03; DOT/FAA/AEE/2020-04). John A. Volpe National Transportation Systems Center, U.S. Department of Transportation. Retrieved from https://rosap.ntl.bts.gov/view/dot/49647

Schäffer, B., Pieren, R., Heutschi, K., Wunderli, J. M., & Becker, S. (2021). Drone noise emission characteristics and noise effects on humans—a systematic review. *Int. J. Environ. Res. Public Health*, *18*(11). Retrieved from https://doi.org/10.3390/ijerph18115940

Sonneborn, W. G. O., & Drees, J. M. (1975). The scissors rotor. *J. Am. Helicopter Soc.*, *20*(3), 18-27. Retrieved from https://doi.org/10.4050/JAHS.20.18

Usov, D., Chronis, T. G., & Filippone, A. (2025, 9). Aerodynamics and Aeroacoustic Response of Low-Reynolds Number Propellers with Unequal Blade Spacing. In *Proceedings of the 51st european rotorcraft forum.* Venice, Italy. Retrieved from https://www.researchgate.net/publication/395454255_Aerodynamics_and_Aeroacoustic_Response_of_Low-Reynolds_Number_Propellers_with_Unequal_Blade_Spacing?utm_source=chatgpt.com

Usov, D., Koning, D., Chronis, T., Filippone, A., Akiwate, D., & Martinez, A. J. T. (2024, 6). Aerodynamics and acoustics of asymmetric propellers with uneven blade spacing. In *30th aiaa/ceas aeroacoustics conference.* Rome, Italy. Retrieved from https://doi.org/10.2514/6.2024-3265

Usov, D., Koning, D., Filippone, A., Poggi, C., & Bernardini, G. (2026). Aeroacoustic response of propellers with unequal blade spacing. *Aerospace Science and Technology*, *168*, 110826. Retrieved from https://doi.org/10.1016/j.ast.2025.110826